Catal Lett (2009) 127:83–94
DOI 10.1007/s10562-008-9634-y

Preparation and Catalytic Performance of Al_2O_3, TiO_2 and SiO_2 Supported Vanadium Based-Catalysts for C–H Activation

Eman Fahmy Aboelfetoh · Rudolf Pietschnig

Received: 6 July 2008 / Accepted: 31 August 2008 / Published online: 15 October 2008

Abstract A series of Al_2O_3, SiO_2 and TiO_2-supported vanadium oxide catalysts with different vanadium loadings has been prepared by two different methods: wet impregnation using ammonium metavanadate as a vanadium precursor and grafting using $VOCl_3$. Characterization of these catalysts by XRD, FTIR, TEM, SEM, EDX, DR and TGA techniques revealed that the structure of vanadium oxide VO_x species depends on the preparation method, the type of the support and loadings of vanadium on the oxides surfaces. Monomeric vanadium oxide species are predominant at low vanadium loadings while polymeric vanadium oxide species increase with higher loadings. The catalytic activity of the prepared catalysts was evaluated for the liquid-phase oxidation of cyclohexane as a model reaction to obtain cyclohexylhydroperoxide, cyclohexanol and cyclohexanone with PCA as co-catalyst. The results show that the catalysts exhibit good cyclohexane conversion and remarkable selectivity to the target products and high turnover numbers (TON).

Keywords Oxide supported catalysts · Selective oxidation · C–H activation · Vanadium

1 Introduction

Catalysts containing vanadium oxides either pure or mixed with other metal oxides are known to be highly efficient catalysts in many homogeneous oxidation reactions [1, 2]. Nevertheless, the use of heterogeneous catalysts offers several advantages such as easy recovery and recycling of catalysts as well as minimization of undesired toxic wastes. Several vanadium based heterogeneous catalysts, e.g., immobilized within a zeolite matrix or attached to various supports, viz., polymers, SiO_2, etc., have been reported to overcome the specific problems of homogeneously catalyzed systems [3–5]. Presently, supported vanadium oxide catalysts are still being intensively studied because of their wide range of applicability in the chemical industry [6–9].

Selective oxidation of cyclohexane to cyclohexanol and cyclohexanone using air/O_2 or other oxidants is the topic of many recent studies [2, 5, 10–15]. These two major products are important intermediates in the manufacturing of nylon-6 and nylon-6,6 polymers and other products [15]. Therefore, a major challenge in this field is to find reaction pathways that afford the primary product with high selectivity, high turnover numbers (TON) at relatively high conversion of the hydrocarbon [2].

The aim of the present study is to provide and to optimize a novel V-based heterogenous catalyst suitable for oxidative C–H functionalization. This includes (1) preparation of different supported vanadium oxide catalysts with different vanadium loading by wet impregnation and grafting techniques, (2) characterization of the prepared catalysts by various techniques and (3) investigation of the catalytic performance of the prepared catalysts in the selective oxidation of cyclohexane in the liquid-phase. This test reaction has already been explored in related studies, e.g., photo-oxidation reactions over V-amorphous support based systems [16] V-MCM-41 based materials [17] and VAPO-5 based materials [18]. One of the issues here is the stability of the material and the potential leaching as well as the re-adsorption on the support.

E. F. Aboelfetoh · R. Pietschnig (✉)
Karl-Franzens-Universität, Institut für Chemie,
Schubertstraße 1, 8010 Graz, Austria
e-mail: rudolf.pietschnig@uni-graz.at

E. F. Aboelfetoh
Faculty of Science, Tanta University, Tanta 31527, Egypt

2 Experimental

Two different methods, grafting and wet impregnation, were applied to prepare supported vanadium oxide catalysts on different support materials such as Al_2O_3, SiO_2 and TiO_2. To remove adsorbed water, the oxide supports were heated at 350 °C for 4 h followed by evacuation at 150 °C for 24 h and subsequent cooling to room temperature under argon atmosphere prior to catalyst preparation. The catalysts were prepared by impregnation of Al_2O_3 (Merck, 99%), TiO_2 (Fluka, 99%) and silica gel 60 (Roth, 98%) with NH_4VO_3 (Fluka, >99%) dissolved in an aqueous solution of oxalic acid (1:2 molar ratio). After impregnation, the samples were dried in air at 100 °C for 24 h and calcined in air at 350 °C for 4 h. Different samples with different V loadings were prepared and designated in the text as ImpnS, where *n* is an integer and S refers to the oxide supports, e.g., for alumina S = Al. For comparison bulk V_2O_5 was freshly prepared by heating ammonium meta vanadate (NH_4VO_3) in air at 450 °C for 4 h.

The incorporation of vanadium to the oxide surfaces by grafting was carried out by refluxing the oxide supports with vanadium oxytrichloride $VOCl_3$ solution in dry *n*-hexane at the boiling point of the solvent (90 °C) for 8 h. The amount of vanadium used for the initial grafting process, roughly corresponds to a monolayer or to moderate excess with respect to a monolayer, by assuming a conventional stoichiometry of one hydroxyl group for one $VOCl_3$ molecule. The relative amount of OH groups on the oxide surfaces was determined by thermogravimetric analysis (TGA). The solid obtained after the initial grafting process was recovered by filtration, washed with dry *n*-hexane several times to remove unreacted $VOCl_3$, dried under vacuum, washed with distilled water to promote the hydrolysis of M–O–Cl bonds and to remove all physisorped vanadium species, dried at 100 °C for 24 h. Some of this dried material was kept under argon as Ungrf1S and finally calcined at 350 °C for 4 h. The same procedure was repeated twice to achieve the desired loading of vanadium on the oxide surfaces. The calcined catalysts are designated in the text as GrfnS, where *n* is the no of grafting processes and S refers to the oxide support.

The vanadium concentration of the prepared catalysts was determined by flame atomic absorption spectroscopy (AAS) using a UNICAM 929 AA spectrometer. The BET surface area of the catalysts was measured by nitrogen adsorption–desorption at 77 K using a NOVA 1200 surface area analyzer (Quanta-chrome). The isotherms were analyzed in a conventional manner in the region of the relative pressure, $p/p_0 = 0.05$–0.3. X-ray diffraction (XRD) patterns of all catalysts were performed on a Philips powder diffractometer PW1050/25 with Cu Kα radiation ($\lambda = 0.1542$ nm) operating at 50 kV and 20 mA in a 2θ range of 10–70° with step size 0.01° and time step 1.0 s to assess the crystallinity of the vanadium oxide loading. The diffractograms of the samples were compared with the powder diffraction patterns of reference samples. Fourier transform-infrared spectra of the samples were recorded on a Perkin–Elmer FT-IR spectrometer 1725× using KBr disks. Diffuse reflectance (DR) spectra in the UV–visible region were recorded in the reflectance function mode ($F(R)$) at room temperature in the range 1,000–200 nm on a Varian Cary 500 spectrophotometer with a diffuse reflectance attachment to investigate the structures of $V(V^{5+})$-containing oxide compounds under inert and hydrated conditions. Each oxide support material was used as a reference for the corresponding supported catalysts. For example Al_2O_3 was used as a reference for alumina supported catalysts (VO_x/Al_2O_3). Thermogravimetric analyses using a Mettler TGA were performed on both support materials and all prepared catalysts. To evaluate the overall amount of surface hydroxyl groups available for anchoring reactions, the weight loss between 300 and 1,000 °C was determined. A heating rate of 10 °C/min under argon was applied to purge off-gasses from the TGA electronics and sample region. The reference material was α-alumina powder. The SEM analyses were done with a DSM 982 Gemini SEM with a maximum acceleration voltage of the primary electrons between 10 and 15 kV. The powder samples were prepared on double side adhesive carbon tape and covered with a gold layer in a Cressington sputter coater operated under vacuum conditions (0.5×10^{-1} mbar). Semi-quantitative EDX (Röntec, M-series, EDR288/SPU2) analysis was used for the characterization of element concentration and vanadium distribution within all prepared catalysts. The TEM examination of samples was carried out on a Philips CM10 microscope working at 100 kV. TEM specimens were prepared ultrasonically by dispersing the catalyst sample in ethanol, and then placing a drop of the suspension on a Cu grid covered with a lacey carbon film.

The catalytic activity of the prepared catalysts was evaluated for the liquid-phase oxidation of cyclohexane as a model reaction to obtain cyclohexylhydroperoxide (Cy–OOH), cyclohexanol (Cy–OH) and cyclohexanone (Cy=O). The catalytic reaction was carried out in a 100 mL round-bottom flask equipped with a reflux condenser under intensive stirring in air at 60 °C using pyrazine 2-carboxylic acid (PCA) as co-catalyst, 30% aqueous H_2O_2 and acetonitrile (CH_3CN) as a solvent. The exact concentration of H_2O_2 is determined before the oxidation reaction by the permanganate method [19]. The catalyst is added first followed by addition of PCA and acetonitrile, the resulting mixture is stirred well for 5 min, after which cyclohexane and hydrogen peroxide are added with continuous stirring. After 24 h the reaction is stopped by cooling with ice, and the catalyst is separated by centrifugation. The products are

identified by GC-MS and their relative amounts are determined directly by its GC peak area using HP 6890 gas chromatography equipped with a split inlet (250 °C, split ratio 50.0) using HP 5 MS capillary column (30 m, 0.25 mm ID; constant flow of carrier gas Helium 1.0 mL/min) coupled to a FID detector.

The catalytic activities are reported as conversion (%), selectivity (%) and TON calculated as follows:

$$\%\,\text{Conversion} = \frac{\%\text{ of the reacted cyclohexane}}{\%\text{ of the starting cyclohexane}} \times 100$$

$$\%\,\text{Selectivity to X} = \frac{\%\text{ of cyclohexane converted to X}}{\%\text{ of reacted cyclohexane}} \times 100$$

where X = cyclohexanol, cyclohexanone and cyclohexylhydroperoxide.

$$\%\ \text{Yield} = \text{The total selectivities of the target products} = (\%S_{\text{CY-OOH}} + \%S_{\text{CY-OH}} + \%S_{\text{CY=O}})$$

TON = moles of cyclohexane converted to the target products per mole of metal (V) in the used amount of catalyst, as determined by AAS.

3 Results and Discussion

3.1 Catalyst Characterization

Tables 1–3 summarize the vanadium content of the catalysts determined from AAS analysis, BET surface areas, VO_x surface densities calculated with the use of these two parameters, and the relative amounts of surface hydroxyl groups of Al_2O_3, TiO_2, SiO_2, VO_x/TiO_2, VO_x/Al_2O_3 and VO_x/SiO_2 catalysts evaluated by TGA. According to earlier studies the weight loss between 300 and 1,000 °C can be attributed only to the loss of hydroxyl groups [20] As a matter of fact, residual chloride groups are eliminated by the hydrolytic step during the grafting process for grafted catalysts and the residual oxalate is eliminated by calcination for impregnated catalysts.

3.1.1 Vanadium Coverage

The initial grafting process of Al_2O_3 with vanadyl trichloride ($VOCl_3$) produces a considerable lower amount of vanadium species (0.45 mmol), as compared to the number of hydroxyl groups (1.80 mmol) on an Al_2O_3 surface. Moreover, the amount of secondary hydroxyl groups on the noncalcined catalyst (Ungrf1Al) is three times higher than that of vanadium ions (Table 1). This result suggests that the secondary hydroxyl groups detected are partly unreacted OH groups of the alumina surface. After calcination a further decrease in the hydroxyl groups of Grf1Al catalyst is noticed, probably due to the interactions of vanadylic species (V-OH) with unreacted OH groups on Al_2O_3 [21, 22] (Scheme 1). The second and third grafting processes increase the amount of grafted vanadium, and consequently decrease the number of hydroxyl groups. This can be mainly attributed to subsequent dehydration of vanadium hydroxide groups during calcinations leading to interconnection of vanadyl groups by V–O–V bonds (Scheme 2). It should be pointed out that schemes 1 and 2 are only intended to illustrate the stoichiometry of immobilization, but do not imply that the coordination of the surface vanadyl species is actually tetrahedral. Additional coordinative bonds with oxygen atoms on the surface may be formed during calcination, especially at higher vanadium concentrations (Scheme 3). Detailed investigations elucidating the actual coordination sphere of the anchored vanadium species have already been performed by Weckhuysen and coworkers for SiO_2, Al_2O_3 and some transition metal oxide supported heterogeneous catalysts [23–25].

Table 1 Characteristics of Al_2O_3-supported vanadium oxide (VO_x/Al_2O_3) catalysts

Catalyst	Color	V content (mmol/g catal.)	OH groups (mmol/g catal.)	Surface area (m^2/g Al_2O_3)	Pore volume cm^3/g catalyst	VO_x surface densities (V atoms/nm^2)	V (wt%)	E_g (eV)
Al_2O_3	White	0.00	1.80	170.67	0.147	–	00.00	–
Ungrf1Al	Green	0.45	1.55	154.09	0.065	1.80	02.30	2.90
Grf1Al	Light yellow	0.49	1.19	171.89	0.114	1.76	02.50	3.24
Grf2Al	Yellow	0.84	0.73	–	–	–	04.28	3.00
Grf3Al	Yellow	0.98	0.67	121.09	0.100	5.14	05.00	2.89
Imp1Al	Light green	0.42	0.82	197.10	0.081	1.31	02.13	3.38
Imp2Al	Yellowish green	0.76	0.57	184.97	0.076	2.56	03.85	3.07
Imp3Al	Yellow	1.20	0.54	135.70	0.053	5.69	06.13	2.90
Imp4Al	Yellow	2.27	0.52	175.25	0.071	8.82	11.55	2.70
VO_x[a]	–	–	–	–	–	–	21.88	2.66

[a] Bulk V_2O_5 diluted with Al_2O_3 (physical mixture of 0.05 g bulk V_2O_5 and 0.1 g Al_2O_3)

Table 2 Characteristics of TiO_2-supported vanadium oxide (VO_x/TiO_2) catalysts

Catalyst	Color	V content (mmol/g catal.)	OH groups (mmol/g catal.)	Surface area (m^2/g TiO_2)	Pore volume cm^3/g catalyst	VO_x surface densities (V atoms/nm^2)	V (wt%)	E_g (eV)
TiO_2	White	0.000	0.070	08.000	0.045	–	0.00	–
Ungrf1Ti	White	0.044	0.111	07.002	0.056	3.78	0.22	2.79
Grf1Ti	White	0.040	0.053	–	–	–	0.20	2.76
Grf2Ti	White	0.045	0.048	–	–	–	0.23	2.73
Grf3Ti	White	0.060	0.041	05.006	0.025	7.22	0.31	2.70
Imp1Ti	White	0.040	0.070	08.016	0.055	3.01	0.20	2.73
Imp2Ti	White	0.060	0.064	08.024	0.053	4.52	0.31	2.73
Imp3Ti	White	0.085	0.032	08.034	0.043	6.40	0.43	2.72
Imp4Ti	Yellowish white	0.200	0.012	–	–	–	1.02	2.63

Table 3 Characteristics of SiO_2-supported vanadium oxide (VO_x/SiO_2) catalysts

Catalyst	Color	V content (mmol/g catal.)	OH groups (mmol/g catal.)	Surface area (m^2/g SiO_2)	Pore volume cm^3/g catalyst	VO_x surface densities (V atoms/nm^2)	V (wt%)
SiO_2	White	0.00	1.05	475.27	0.410	–	00.00
Ungrf1Si	Dark green	0.36	1.34	509.44	0.441	0.43	01.82
Grf1Si	White	0.36	0.78	451.98	0.378	0.48	01.82
Grf2Si	White	0.21	0.75	–	–	–	01.06
Grf3Si	White	0.18	0.82	–	–	–	00.92
Imp1Si	White	0.21	0.65	–	–	–	01.06
Imp2Si	White	0.36	0.79	428.43	0.372	0.51	01.82
Imp3Si	Yellowish orange	1.08	0.62	318.52	0.275	2.16	05.50
Imp4Si	Yellowish orange	2.55	–	–	–	–	13.00
Imp5Si	Orange	3.50	–	271.26	0.225	9.45	17.82

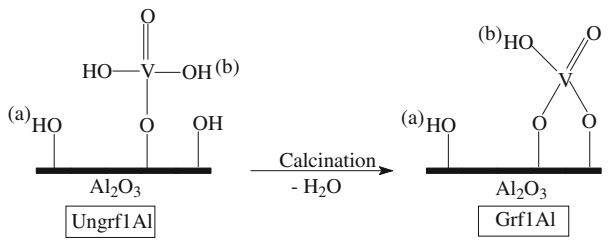

Scheme 1 Interconnection between the vanadylic species (V-OH) and unreacted OH groups of Al_2O_3 during calcination with **a** unreacted hydroxyl groups on an Al_2O_3 surface and **b** secondary hydroxyl groups

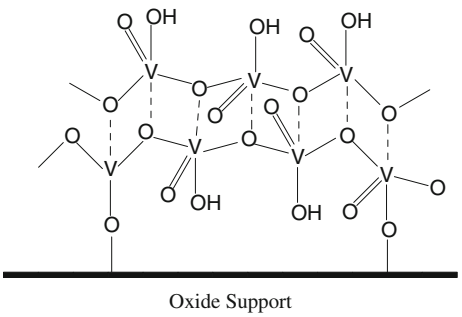

Scheme 3 Interconnection of vanadyl groups

Scheme 2 Dehydration of vanadium hydroxide groups during calcination

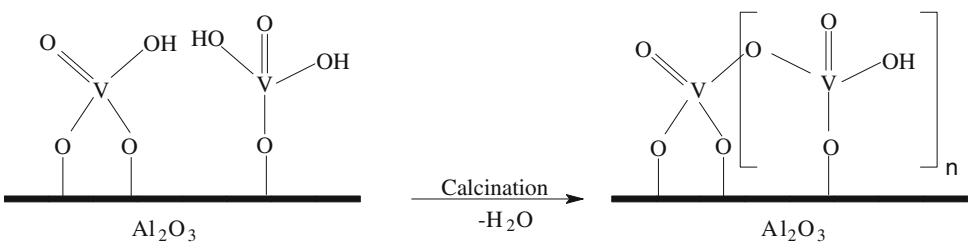

On a titania surface, the amount of vanadium deposited in the initial grafting process matches about 62.8% of the total amount of hydroxyl groups (Table 2). Therefore, the high amount of secondary hydroxyl functionalities on the noncalcined catalyst (Ungrf1Ti) corresponds to unreacted hydroxyl groups. After calcination, the catalyst shows a decrease in the amount of hydroxyl functions (Grf1Ti), due to interactions of vanadylic species (V-OH) with the unreacted OH groups on TiO_2 [21, 22]. Repeating the grafting process, slightly increases the amount of grafted vanadium and decreases the number of hydroxyl groups by 22.6%, which can be attributed to the increased interconnection of vanadyl groups under formation of V–O–V bonds (Schemes 2 and 3). For silica supported catalysts the situation is quite different. Here, the amount of grafted vanadium actually decreases by repeating the grafting process (Table 3). The reason for this is likely to be leaching of vanadium oxide from the silica surface during the hydrolytic step of the grafting process, which underlines the reversible nature of the anchoring process.

3.1.2 Determination of Surface Area

The BET surface areas per gram of Al_2O_3 and the pore volumes are decreased with increasing vanadium loading for impregnated or grafted catalysts, while a considerable increase in surface area is found for Imp4Al (175.25 m^2/g) with the highest loading. This trend reflects the presence of vanadium oxide as separate particles without pore blocking [26]. Similarly, the surface areas per gram of SiO_2 decrease as the V loading is increased. The decrease of pore volumes also suggests the formation of larger V_2O_5 crystallites that block some pores of the support material [27]. The surface areas per gram of TiO_2 of the impregnated VO_x/TiO_2 catalysts Imp1Ti, Imp2Ti and Imp3Ti are approximately equal. This trend corresponds to the low surface area of the added VO_x.

3.1.3 Monolayer Surface Coverage

Monolayer surface coverage of polymerized VO_4 species on different oxide supports has been determined before by Raman spectroscopy and was found to be approximately 7–8 V-atom/nm^2 [28, 29]. At low VO_x surface densities (2.3–2.5 V-atom/nm^2), monovanadate species (VO_4) are predominant irrespective of the support material [22]. On the contrary, silica-supported vanadium oxide exhibits a maximum surface coverage of polymerized VO_4 species at about 2 V-atom/nm^2 [30]. The lower monolayer surface coverage on silica is explained by the lower density and reactivity of the silica surface hydroxyls [31]. Above monolayer coverage particles of V_2O_5 are formed [30].

3.1.4 Characterization with X-ray Diffraction

The XRD patterns of the VO_x/Al_2O_3 catalysts with loadings up to 6.13 wt% V prepared by either grafting or impregnation show only the characteristic peaks of the Al_2O_3. The support is mostly γ-Al_2O_3 with well-defined peaks at $2\theta = 67.3°$, 45.7° and 37.3° corresponding to ($d = 1.4$, 2.0, and 2.4 Å) [32], while some additional small peaks indicate the presence of a minor amount of δ-Al_2O_3 at $2\theta = 57.5°$, 43.4°, 25.5° and 35.2° [33]. For the impregnated catalyst (Imp4Al) with high V loading of 11.55 wt%, besides the typical peaks of Al_2O_3 well-defined peaks at $2\theta = 15.5°$, 20.0°, 21.5°, 26.0°, 31.0°, 32.5° and 34.0° appear, which correspond to crystalline V_2O_5. The presence of TiO_2 (anatase) at $2\theta = 25.3°$, 37.1°, 37.8°, 38.6°, 48.1°, 54.0°, 55.0°, 62.8° and 68.9° is detected as the only crystalline phase both in the grafted and impregnated VO_x/TiO_2 catalysts. The XRD patterns of VO_x/SiO_2 catalysts show a peak at about $2\theta = 22.3°$, which is broadened due to the partially amorphous nature of silica. Grafted and impregnated silica samples, both with low loadings, only show this characteristic SiO_2 reflex, indicating that the vanadium oxide is well dispersed on the surface of the support with a crystal size below the detection limit of the method [34]. In contrast, silica impregnated vanadium oxide with high loadings, such as Imp4Si and Imp5Si catalysts show peaks at $2\theta = 15.3°$, 20.0°, 21.2°, 25.9°, 30.9°, 32.1° and 34.1°, in addition to the characteristic silica peak. The intensity of these additional peaks increases from Imp4Si to Imp5Si and are attributed to the presence of crystalline vanadium pentoxide V_2O_5.

3.1.5 Characterization with IR Spectroscopy

The FT-IR spectra of the VO_x/Al_2O_3 catalysts of 2.13–6.13 wt% V prepared by grafting or impregnation are dominated by the characteristic features of Al_2O_3. In contrast, impregnated catalyst Imp4Al with a high loading of V (11.55 wt%) shows the characteristic bands of crystalline V_2O_5 at 1,025 and 816 cm^{-1} (Fig. 1). These bands correspond to the V=O stretching and the V–O–V bending modes, respectively [35]. With FT-IR the characteristic band of vanadium oxide (V=O) in the catalysts with loadings lower than Imp4Al (11.55 wt%) was not easy to identify. This might be a consequence of the high dispersion of vanadium oxide on the surface as well as the low concentration of vanadium oxide. Similarly, impregnated and grafted VO_x/TiO_2 catalysts do not exhibit any bands characteristic for crystalline V_2O_5. The VO_x/SiO_2 catalysts prepared by grafting and impregnation with different loadings display the characteristic bands of silica at 450, 804, 1,080, 1,624 and 3,424 cm^{-1}. The band at 804 cm^{-1} is characteristic for a symmetric ν(Si–O–Si) stretching

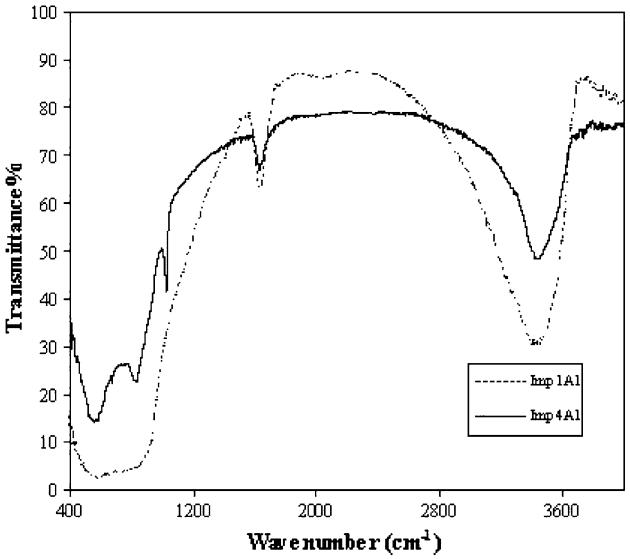

Fig. 1 FT-IR spectra of Imp1Al (2.13 wt%V) and Imp4Al (11.55 wt% V) catalysts

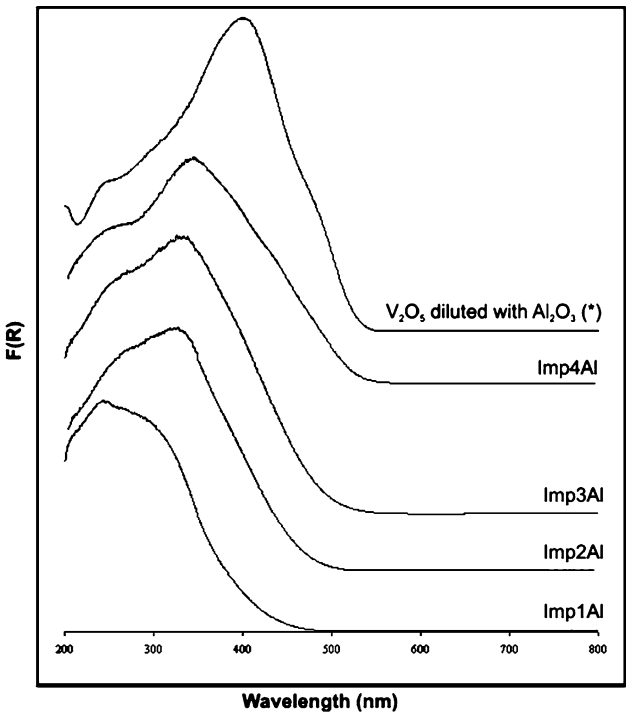

Fig. 2 DR-UV–Visible spectra of impregnated (VO_x/Al_2O_3) catalysts under inert conditions

vibration, and the band at 1,080–1,220 cm^{-1} [36] is characteristic for an asymmetric ν(Si–O–Si) stretching vibration. The silica impregnated catalysts with high V loadings exhibit a very weak band at 955 cm^{-1}, which indicates an asymmetric stretching mode of Si–O–V [37]. This band is detectable and its intensity increases with the vanadium content from the Imp4Si to the Imp5Si catalyst. The presence of the characteristic band of V_2O_5 is not easily identified by IR spectroscopy, because the silica absorption bands overlap with the vibrations of the surface vanadium oxide species [31].

3.1.6 Characterization with UV–Vis Spectroscopy

The diffuse reflectance UV–visible spectra of VO_x/Al_2O_3 catalysts either grafted or impregnated under water free conditions exhibit broad bands below ~550 nm, characteristic of charge transfer transitions from oxygen to vanadium (V^{5+}) [38–40]. The spectrum of Imp1Al shows a broad band at about 251 nm. The spectrum observed for Imp2Al exhibits a small band around 325 nm. This band is found to grow and shift with increasing V loading to 333 and 343 nm for Imp3Al and Imp4Al, respectively (Fig. 2). The observed red shift and the relative increase of the band at 325 nm suggest a higher degree of condensation and therefore, an increase in the amount of oligomeric vanadium oxide species at higher loading. On the other hand grafted (VO_x/Al_2O_3) catalysts show broad bands around 309 nm for the noncalcined catalyst (Ungrf1Al) and of 301 nm for calcined catalyst (Grf1Al) obtained from the initial grafting process. By repeating the grafting process the broad band at 301 nm is increased and shifted to 331 nm for Grf2Al and to 338 nm for Grf3Al. This implies an increase of the degree of polymerization of the vanadium oxide species by repeating the grafting process.

Previously, the edge energy values have been used to characterize different VO_x containing compounds [32, 40], the edge energy for the catalysts are determined from the intercept of a *straight* line fitted through the rise of the function $[F(R)\ h\nu]^2$ plotted versus $h\nu$ [41], where $F(R)$ is a Kubelka–Munk function and $h\nu$ is the energy of the incident photon.

The edge energy values of impregnated and grafted VO_x/Al_2O_3 catalysts under inert conditions are determined (Table 1). These values indicate that the impregnated catalyst (Imp1Al) with low loading shows an edge energy of 3.38 eV. The increase of the V loading to 11.55% (Imp4Al) decreases the edge energy of the surface vanadium oxide species further to 2.70 eV. A high edge energy value of about 3.38 eV is attributed to V^{5+} in isolated VO_4 species [32, 40], while the low value of 2.70 eV is in close proximity to the energy edge value (2.66 eV) of bulk V_2O_5 diluted with Al_2O_3 (Fig. 2). The decrease in E_g values with increasing V loadings refers to the presence of polymerized VO_4 or polymerized VO_5/VO_6 [40]. In control experiments we found for VO_x/Al_2O_3 that there is no pronounced change of E_g values of impregnated catalysts upon air exposure. The same behavior is found for the other grafted Al_2O_3-supported catalysts. This stability is already indicated by the color of the catalysts, which does not change upon air exposure.

The DR spectra for VO_x/TiO_2 catalysts show sharp absorption bands in the range of 350–515 nm with a maximum at 400 nm. Also, the edge energies of the surface vanadium oxide species of impregnated and grafted catalysts are variable between 2.63 and 2.79 eV (Table 2) irrespective of the V loading. The strong support absorption in the higher energy region overlaps the weak absorption from a small amount of vanadium (V^{5+}) cations of the same wavelengths [40].

The DR spectra of VO_x/SiO_2 catalysts (impregnated and grafted) under inert conditions show only a single band (Fig. 3), indicating that the vanadium oxide species are well dispersed in these samples. The band maxima are ranging from 266 to 300 nm and the corresponding edge energies are ranging from 3.86 to 3.12 eV with increasing loading from 00.92 to 17.82 wt% V (Table 4). The high E_g values are due to isolated VO_4 species. The impregnated catalysts with low loadings (Imp1Si and Imp2Si) exhibit remarkably high edge energies of 3.76 and 3.74 eV compared to other isolated VO_4 structures [32, 40]. An explanation for these findings might be the high distortion of the VO_4 structure. The presence of a small amount of V_2O_5 crystallites may be responsible for the slightly lower E_g values of Imp4Si (3.26 eV) and Imp5Si (3.12 eV). Moreover, the grafted sample obtained from the initial grafting process before calcination (Ungraf1Si) exhibits a low edge energy (2.51 eV) compared to the identical sample (Grf1Si) after calcination, which might be explained by the ligand effect. This means the calcination process changes the local structure of vanadium oxide by changing the relative ratio of $VO_2(OH)_2$ to $VO_3(OH)$ on the silica surface. All catalysts samples either grafted or impregnated exhibit broad bands below ~550 nm, due to charge transfer transitions from oxygen to vanadium (V^{5+}), as described above.

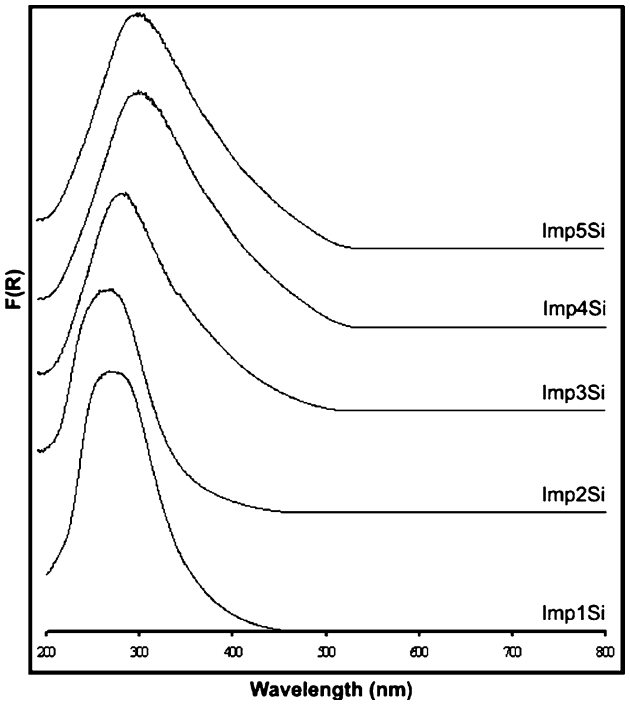

Fig. 3 DR-UV–Visible spectra of impregnated (VO_x/SiO_2) catalysts under inert conditions

Table 4 Comparison of UV–vis absorption maxima and edge energy values of VO_x/SiO_2 catalysts under inert[a] and hydrated[b] conditions

Catalyst	Band max. (nm)[a]	E_g (eV)[a]	Band max. (nm)[b]	E_g (eV)[b]
Imp1Si	266	3.76	279 & 362	2.79
Imp2Si	270	3.74	279 & 362	2.78
Imp3Si	287	3.46	291–387	2.72
Imp4Si	300	3.26	291–387	2.68
Imp5Si	300	3.12	287–348 & 448 (sh)	2.66
VO_x[c]	–	–	295 & 377 & 480 (sh)	2.66
Ungrf1Si	296–390	2.51	287–377	2.42
Grf1Si	285	3.6	287–377	2.66
Grf2Si	272	3.76	287–356	2.86
Grf3Si	266	3.86	279	3.01

sh = shoulder

[a] Water free VO_x/SiO_2

[b] Hydrated VO_x/SiO_2 catalysts

[c] Bulk V_2O_5 diluted with SiO_2 (physical mixture of 0.05 g bulk V_2O_5 and 0.1 g SiO_2)

The effect of hydration on the dispersion and molecular structure of vanadium oxide species of the catalyst surfaces was studied after 3 h of air exposure of water free (VO_x/SiO_2) samples. The impregnated catalysts with low loading such as Imp1Si and Imp2Si show two broad bands at 279 nm and 362 nm. This observation suggests that some of the isolated monovanadate VO_4 is still present but the major part of this species is transformed to square pyramidal or octahedral V species (poly VO_5/VO_6) [42]. In contrast the impregnated catalysts with high loadings exhibit broad bands in the range of 291–387 nm, suggesting the presence of highly polymerized species of VO_5/VO_6 (Fig. 4). This is in good agreement with the E_g values of the hydrated VO_x/SiO_2 catalysts, where lower E_g values are observed than in water free catalysts (Table 4).

3.2 Catalytic Activity

3.2.1 Previous Studies

The commercial process to produce cyclohexanol and cyclohexanone on an industrial scale starting from cyclohexane and molecular oxygen is to use cobalt salts as catalysts, which gives ca. 4% conversion and 70–85% selectivity at 150 °C under 1–2 MPa pressure [15]. Many

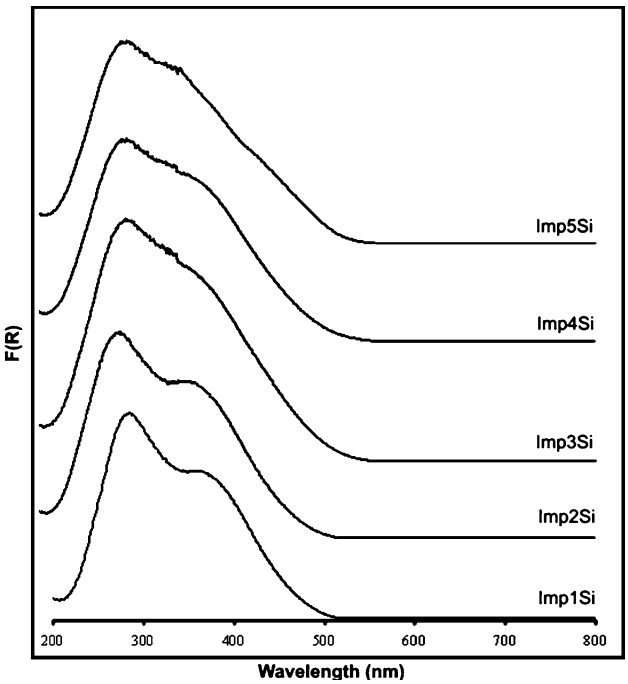

Fig. 4 DR-UV–Visible spectra of impregnated (VO_x/SiO_2) catalysts after 3 h air exposure

attempts have been made to improve or substitute the classical process by developing heterogeneous catalysts with oxygen or peroxides as nonpolluting oxidants under mild conditions [2, 5, 10–15]. The most interesting applied processes using oxidants such as hydrogen peroxide, *tert*-butyl hydroperoxide (*t*-BHP) and molecular oxygen are listed in Table 5.

3.2.2 Catalytic Activity Measurements

We investigated the catalytic activity of the catalysts prepared by us as described in Sect. 2. According to the catalytic activity measurements, the primary oxidation products of cyclohexane (Cy–H) are the corresponding cyclohexylhydroperoxide (Cy–OOH) as well as small amounts of a mixture of cyclohexanol (Cy–OH) and cyclohexanone (Cy=O). The effect of various factors such as vanadium loading, vanadium distribution, catalyst amount, hydrogen peroxide concentration and reaction time on conversion, selectivity and TON has been investigated to obtain the optimum reaction conditions.

3.2.2.1 Effect of Vanadium Distribution A considerable increase in the conversion of cyclohexane with increasing V loadings is noted by applying the same surface area (ca. 0.22 m^2) of impregnated or grafted catalysts of VO_x/TiO_2. However, the TON and the selectivity to Cy–OOH of these catalysts decrease with increasing V loadings (Fig. 5). This observation suggests that the highly polymerized species of vanadium oxide in catalysts containing high loadings such as Grf3Ti and Imp3Ti catalysts accelerate the overoxidation of Cy–OOH to unwanted by-products such as 1,4-cyclohexanedione, 1,3-cyclohexanediol, 4-hydroxy-cyclohexanone, 2-hydroxy-cyclohexanone and 2,4-dihydroxy-cyclohexanone, which could be identified by mass spectrometry.

3.2.2.2 Effect of Catalyst Amount High TONs and selectivities to Cy–OOH are obtained by low amounts of the catalysts (Table 6). Further increases of the catalyst

Table 5 Cyclohexane oxidation by different catalytic systems

Catalyst	Reaction conditions	Conv. %	Products selectivity	References
Ce/Y (zeolites) (Si: Al = 12.5)	*t*-BHP (oxidant) at 70 °C after 24 h	07.6	49% to Cy–OH, Cy=O and cyclohexene	[10]
Salen vanadium (VI) complex/carbamated silica gel	200 °C and 23.8 atm (350 psi) pressure after 16 h	13.0	79.3% to Cy–OH and Cy=O	[11]
Co/TUD-1[a]	*t*-BHP(oxidant) and chlorobenzene at 70 °C after 16 h	10.4	~80% to Cy–OH, Cy=O, Cy–OOH, cyclohexyltertbutyl ether and cyclohexylformate	[12]
$MnP/VOPO_4$	Dichloroethane (solvent) and iodosylbenzene (oxidant), at room temp. after 24 h	10.0[b]	Not determined	[13]
$FeP/VOPO_4$		12.0[c]	Not determined	
FeCoMnAPO-5	*t*-BHP, O_2 (1.0 Mpa), 130 °C after 3 h	06.8	69.7% to Cy–OH, Cy=O and Cy–OOH	[14]
Ag/MCM-41	O_2 (1.4 Mpa), 140 °C after 3 h	08.6	85% to Cy–OH, Cy=O and Cy–OOH	[15]
Maltolato vanadium (V)complex/silica gel	Cyclohexane (4.8 mmol), CH_3CN (5 ml), H_2O_2 (20 mmol), PCA (20 × 10 mmol) at 50 °C after 14 h	25.0	Not determined	[5]

Note: Cy–OOH = cyclohexylhydroperoxide, Cy–OH = cyclohexanol, Cy=O = cyclohexanone

[a] Cobalt-incorporated mesoporous silica with Si/Co ratio of 108

[b] To cyclohexanol

[c] To cyclohexanone

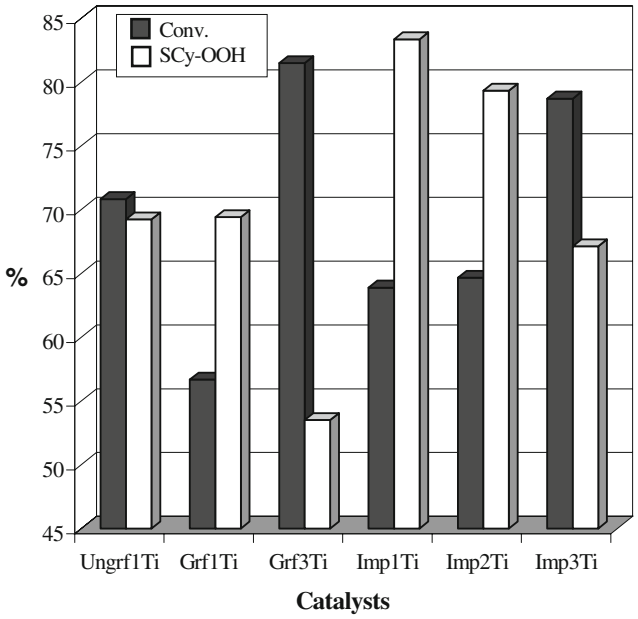

Fig. 5 Variation of cyclohexane conversion and selectivity to Cy–OOH using different VO_x/TiO_2 catalysts with the same surface area (ca. 0.22 m^2)

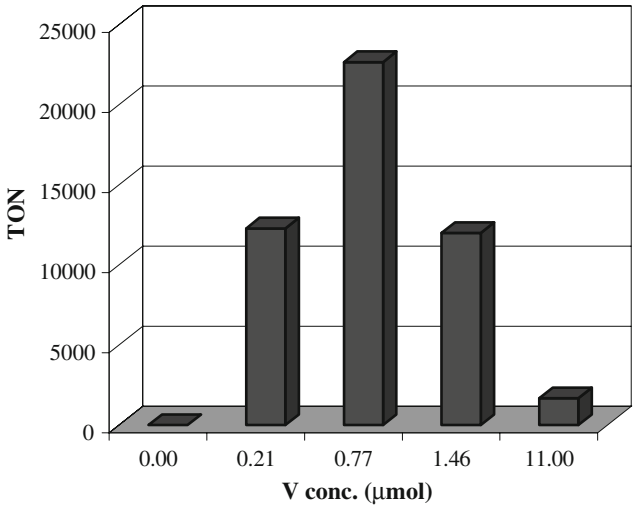

Fig. 6 Variation of TON with different amounts of Ungrf1Si catalyst

amounts (e.g., Ungrf1Si and Grf1Ti) significantly increase the conversion of cyclohexane, while the TON and the selectivity to Cy–OOH decrease in the same order (Figs. 6, 7). The total selectivity to the target products (yield) decreases as well. This effect may be due to the liberation of uncomplexed V^{5+}, which is prone to decompose H_2O_2 instead of reacting with cyclohexane. Furthermore, this uncomplexed species accelerates the oxidation of Cy–OOH to unwanted by-products.

3.2.2.3 Effect of Reaction Time Owing to its high TON, Grf1Ti catalyst has been selected to study the effect of time on the conversion and product selectivity. The conversion and turnover numbers are increased with reaction time and reach a maximum after 48 h with 66.5% conversion and 30,964 TON. Further increase of the reaction time to 96 h a decrease in conversion to 61.1% is detected. Moreover, for reaction times exceeding 48 h a slight decrease of the yield is obtained. The reason for this finding is probably based on the counterplay of several different effects. Blocking of active sites or pores on the catalyst surface may occur by adsorption of reaction products at long reaction times. In principle, this should result in a saturation curve, however, no drop of activity below a steady level should be observed. Additional aspects accounting for the further

Table 6 Oxidation of cyclohexane with different vanadium oxide supported catalysts

Catalysts	V conc. (μmol V)	% Conv.	TON	% S_{Cy-OH}	% $S_{Cy=O}$	% S_{Cy-OOH}	% Yield	% By-pro.	% Leaching
Grf1Ti	0.57	56.68	263,990	11.10	15.70	69.41	96.21	2.15	02
Grf3Ti	0.57	44.91	204,880	17.85	27.71	48.66	94.22	2.59	09
Grf1Ti[a]	0.57	71.10	30,818	11.66	16.77	61.10	89.53	7.44	–
Grf1Si	0.77	61.43	21,348	09.34	12.02	75.96	97.32	1.65	100
Imp2Si	0.77	50.20	17,365	09.93	09.37	77.58	96.88	1.57	100
Imp1Al	1.52	58.01	101,249	07.91	11.36	75.80	96.07	2.27	05
Imp3Al	1.52	61.44	10,505	10.85	14.06	69.20	94.12	3.61	09
Imp4Al	1.52	62.79	9,998	13.46	17.47	56.72	87.65	7.75	20
Grf1Al	2.16	65.46	8,180	03.96	11.20	82.67	97.82	–	03
Grf3Al	1.52	59.43	10,790	10.74	16.04	70.00	96.78	1.91	07
V_2O_5	0.77	30.91	10,622	07.67	11.70	76.53	95.90	1.27	100

Reaction conditions: Cyclohexane (1.06 M, 27.56 mmol), H_2O_2 (0.40 M, 10.5 mmol), PCA (1.70×10^{-3} M, 0.044 mmol), CH_3CN (20 ml), 60 °C, 24 h. % By-products: 1,4-cyclohexanedione, 1,3-cyclohexanediol, 4-hydroxy-cyclohexanone, 2-hydroxy-cyclohexanone, 2,4-dihydroxy-cyclohexanone

[a] The same reaction conditions except H_2O_2 = (0.86 M, 22.36 mmol)

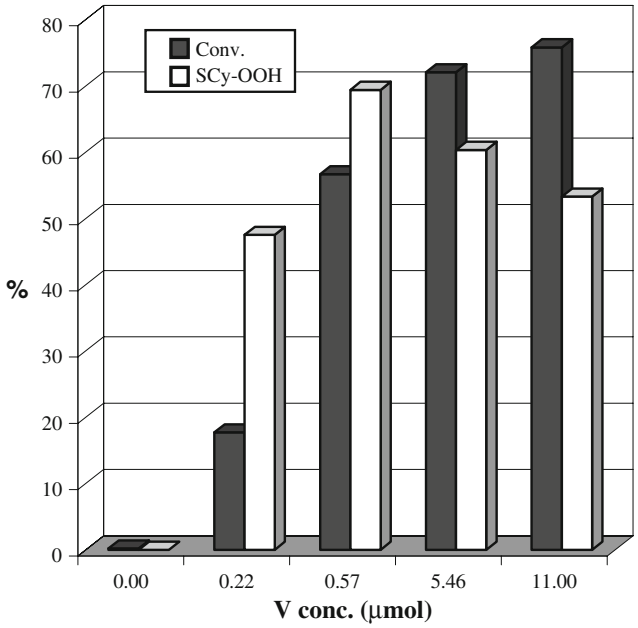

Fig. 7 Variation of cyclohexane conversion and selectivity to Cy–OOH with different amounts of Grf1Ti catalyst

drop at prolonged reaction times may include overoxidation, of product, leaching of the active species, etc.

3.2.2.4 Effect of H_2O_2 Concentration The effect of the H_2O_2 conc. has been assessed using catalysts Grf1Ti and Grf1Al (Table 6 and Fig. 8). The conversion of cyclohexane increases with increasing H_2O_2 concentration, while the selectivity to Cy–OOH and the yield decrease. This shows that the higher conc. of H_2O_2 accelerates the overoxidation of Cy–OOH to unwanted by-products and the total selectivity to the target products (yield) decreases.

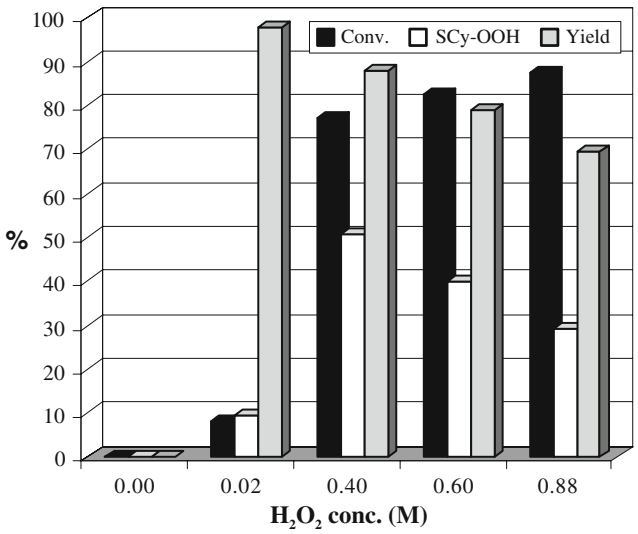

Fig. 8 Variation of the cyclohexane conversion and selectivity to Cy–OOH and the total selectivity to the target products (Yield) with different conc. of H_2O_2 using Grf1Al catalyst (44 µmol V)

3.2.2.5 Stability of the Catalysts to Leaching Under reaction conditions (Table 6), grafted or impregnated catalysts with low vanadium loadings (Grf1Ti, Grf1Al, Imp1Al, Imp1Ti) show a slight leaching (2–5%) of vanadium as confirmed by UV analysis. Catalysts with high loading such as Grf3Ti, Imp3Ti, Grf3Al, Imp3Al and Imp4Al show partial leaching (9–20%). This increased leaching may be explained by the presence of highly polymerized species of vanadium oxide (V_2O_5) in these catalysts, which is completely soluble in the reaction mixture forming homogenous solutions. These findings are in good agreement with results of SEM and TEM measurements where at low vanadium loadings for the Al_2O_3- and TiO_2-based catalysts (either impregnated or grafted) a homogenous distribution of V on the surface is confirmed by EDX. Such a homogenous distribution seems to be more robust against leaching. By contrast at high vanadium loadings, the Al_2O_3- and less pronounced the TiO_2-based catalysts (impregnated more than grafted) show according to SEM/TEM characteristic needle-like crystals of V_2O_5 at the catalyst surface which are prone to leaching (Figs. 9, 10).

Even worse is the situation for VO_x/SiO_2 catalysts, for which vanadium is leached completely from the catalysts surface and therefore can not be recovered by centrifugation. This behavior again is in good agreement with the SEM results which reveal the presence of thin needle crystals of V_2O_5 (up to 100 nm diameter) on the support surface even of the grafted SiO_2 based catalyst with the lowest vanadium loading, Grf1Si (Fig. 9b). According to our findings leaching of vanadium is lowest for TiO_2 based supports and highest for SiO_2 based ones. Moreover, attachment of vanadium via grafting reduces leaching compared to impregnation. These trends are well followed by our SEM/TEM results where the presence of crystalline V_2O_5 phases corresponds to high leaching rates. Although some of the leaching rates for our catalysts are quite substantial, they are still lower than those observed for related catalysts in the literature which amount to 25–33% leaching [18].

3.2.2.6 Effect of PCA Concentration The addition of PCA has a significant influence on the conversion of cyclohexane. It coordinates easily with Lewis acid sites on the catalyst surface (vanadium site) forming a V^{V}(PCA) complex on the catalysts surface. In the presence of hydrogen peroxide a V^{VI}(PCA) complex is formed and hydroxyl radicals ($HO^{\bullet}$) are generated (Eqs. 1–3) [5, 43, 44]. This mechanism of free radical generation was suggested based on a density functional theory study (DFT) [45]. The attack of hydroxyl radicals on cyclohexane produces cyclohexyl radicals. The latter rapidly react with molecular

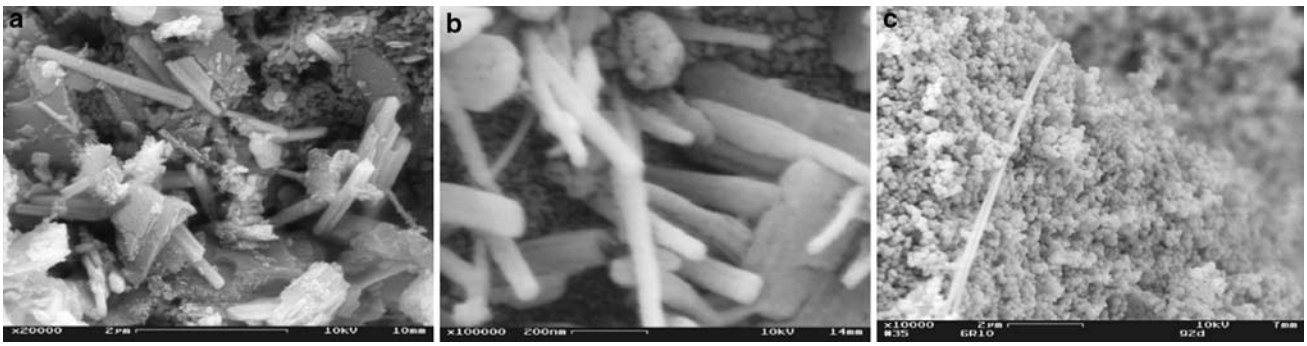

Fig. 9 SEM micrographs of **a** Imp4Al catalyst (11.55 wt%V), **b** Grf1Si catalyst (1.82 wt%V) and **c** Imp4Ti (1.02 wt%V)

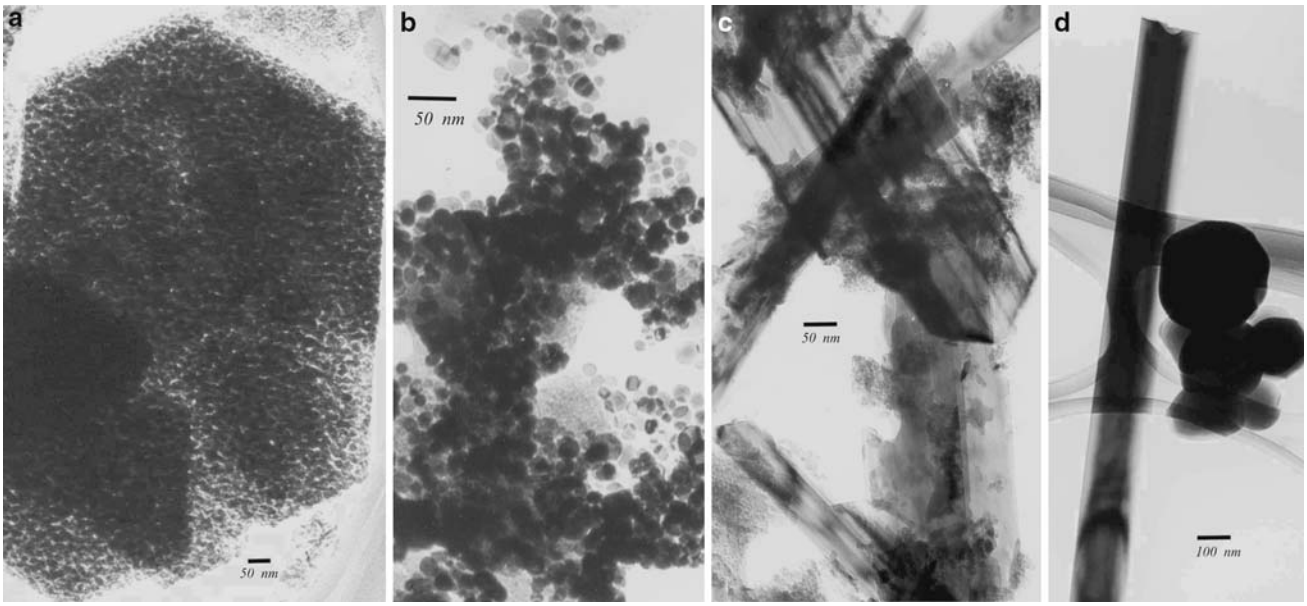

Fig. 10 TEM micrographs of Al_2O_3 crystals (**a**), Imp4Al catalyst (11.55 wt% V) showing aggregates (**b**) and crystals of V_2O_5 (**c**) and Imp4Ti catalyst (1.02 wt% V) showing the presence of needle-like crystals of V_2O_5 (**d**)

atmospheric oxygen. Cyclohexylhydroperoxyl radicals, thus formed can be converted to cyclohexylhydroperoxides. Increasing the conc. of PCA clearly improves the performance of the catalysts. A further increase of PCA decreases the total selectivity of the target product (Fig. 11). The proposed role of PCA is to facilitate the proton transfer between the oxo or hydroxy ligands of the vanadium complex and molecules of hydrogen peroxide or water [44]. In agreement with the above mechanism, we did not find catalytic activity for our catalysts in the absence of molecular oxygen.

$$V^{V}(PCA)(H_2O_2) \rightarrow V^{IV}(PCA) + HOO^{\bullet} + H^{+} \quad (1)$$

$$V^{IV}(PCA) + H_2O_2 \rightarrow V^{V}(PCA) + HO^{\bullet} + HO^{-} \quad (2)$$

$$V^{V}(PCA)(H_2O_2) + HOO^{\bullet} \rightarrow V^{V}(PCA) + HO^{\bullet} + H_2O + O_2 \quad (3)$$

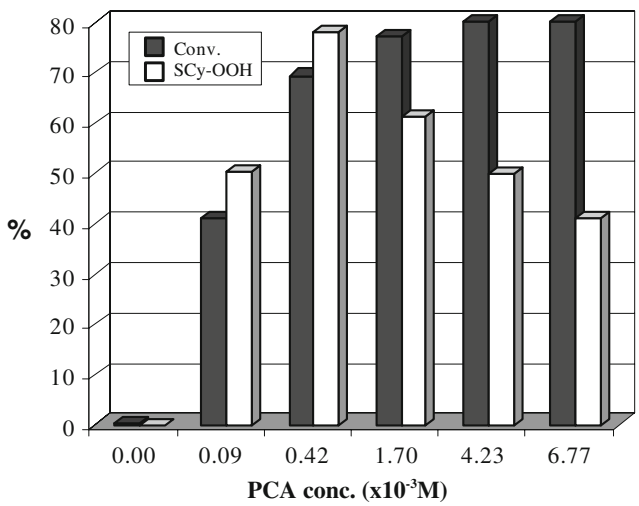

Fig. 11 Variation of cyclohexane conversion and selectivity to Cy–OOH with PCA conc. using Imp1Ti catalyst (11 μmol V)

4 Conclusions

Structural and surface characterization of VO_x/Al_2O_3, VO_x/TiO_2 and VO_x/SiO_2 catalysts shows that the molecular structure of VO_x species depends on the preparation method, the type of the support and loading of vanadium on the oxide support. Monomeric vanadium oxide species are predominant at low vanadium loadings while polymeric vanadium oxide species dominate with increasing vanadium loadings.

Our results show that the catalysts prepared by us exhibit significant activity in the oxidation of cyclohexane. The catalytic activity remarkably depends on the molecular structure of vanadium oxide species. High selectivities to the target products (Cy–OOH, Cy–OH and Cy=O) as well as TON are observed for the highly isolated vanadium oxide species (VO_4) present for instance on TiO_2 supports prepared by grafting. An explanation for this might be that the polymerized vanadium oxide species (VO_4, VO_5/VO_6) on other supports beside their high activities for the cyclohexane also accelerate the overoxidation of Cy–OOH to unwanted by-products, so that the total selectivity to the target products decreases. Also high concentrations of H_2O_2 should be avoided to achieve high conversion rates, because again overoxidation of Cy–fOOH to unwanted by-products occurs.

Acknowledgments The authors would like to thank the Austrian Academic Exchange Service (ÖAD) for financial support for E.F.A during her Ph.D studies and the Austrian Science Fund (FWF) for continued funding (P17882-N11).

References

1. Süss-Fink G, Gonzalez L, Shul'pin GB (2001) Appl Catal A Gen 217:111–117
2. Pillai UR, Sahle-Demessie E (2003) New J Chem 27:525–528
3. Lee JS, Park ED (2002) Top Catal 18:67–72
4. Maurya MR, Saklani H, Kumar A, Chand S (2004) Catal Lett 93:121–127
5. Shul'pin GB, Mishra GS, Shul'pina LS, Strelkova TV, Pombeiro AJL (2007) Catal Commun 8:1516–1520
6. Bautista FM, Campelo JM, Luna D, Luque J, Marinas JM (2006) Catal Today 112:28–32
7. Kus′trowski P, Segura Y, Chmielarz L, Surman J, Dziembaj R, Cool P, Vansant EF (2006) Catal Today 114:307–313
8. Liu W, Lai SY, Dai H, Wang S, Sun H, Au CT (2008) Catal Today 131:450–456
9. Launay H, Loridant S, Nguyen DL, Volodin AM, Dubois JL, Millet JMM (2007) Catal Today 128:176–182
10. Pires EL, Magalhaes JC, Schuchardt U (2000) Appl Catal A Gen 203:231–237
11. Mishra GS, Kumar A (2002) Catal Lett 81:113–117
12. Anand R, Hamdy MS, Hanefeld U, Maschmeyer T (2004) Catal Lett 95:113–117
13. Zampronio EC, Gotardo MCAF, Assis MD, Oliveira HP (2005) Catal Lett 104:53–56
14. Zhou L, Xu J, Miao H, Li X, Wang F (2005) Catal Lett 99: 231–234
15. Zhao H, Zhou J, Luo H, Zeng C, Li D, Liu Y (2006) Catal Lett 108:49–54
16. Teramura K, Tanaka T, Yamamoto T, Funabiki T (2001) J Mol Catal A 165:299–301
17. Dapurkar SE, Sakthivel A, Selvam P (2004) J Mol Catal A 223:241–250
18. Fan W, Fan B, Song M, Chen T, Li R, Dou T, Tatsumi T, Weckhuysen BM (2006) Microporous Mesoporous Mater 94:348–357
19. Jeffery GH, Bassett J, Mendham J, Denney RC (1989) Vogel's text book of quantitative chemical analysis. Longman, London
20. Wilson P, Madhusudhan Rao P, Viswanath RP (2003) Thermochim Acta 399:109–120
21. Weckhuysen BM, Keller DE (2003) Catal Today 78:25–46
22. Sorrentino A, Regaa S, Sannino D, Magliano A, Ciambelli P, Santacesaria E (2001) Appl Catal A Gen 209:45–57
23. Keller DE, Visser T, Soulimani F, Koningsberger DC, Weckhuysen BM (2007) Vib Spectrosc 43:140–151
24. Keller DE, Koningsberger DC, Weckhuysen BM (2006) J Phys Chem B 110:14313–14325
25. Keller DE, de Groot FMF, Koningsberger DC, Weckhuysen BM (2005) J Phys Chem B 109:10223–10233
26. Jonson B, Rebenstorf B, Larsson R, Andersson SLT (1988) J Chem Soc Faraday Trans 84:1897–1910
27. Argyle MD, Chen K, Bell AT, Iglesia E (2002) J Catal 208: 139–149
28. Barbero BP, Cadus LE (2003) Appl Catal A Gen 244:235–249
29. Kustov AL, Kustova MY, Fehrmann R, Simonsen P (2005) Appl Catal B Environ 58:97–104
30. Janssens J-P, van Langeveld AD, Moulijn JA (1999) Appl Catal A Gen 179:229–239
31. Wachs IE, Weckhuysen BM (1997) Appl Catal A Gen 157:67–90
32. Shiju NR, Anilkumar M, Mirajkar SP, Gopinath CS, Rao BS, Satyanarayana CV (2005) J Catal 230:484–492
33. Harlin ME, Niemi VM, Krause AOI (2000) J Catal 195:67–78
34. Kanervo JM, Harlin ME, Krause AOI, Bañares MA (2003) Catal Today 78:171–180
35. Sohn JR, Seo KC, Pae YI (2003) Bull Korean Chem Soc 24: 311–317
36. Dutoit DCM, Schneider M, Fabrizioli P, Baiker A (1996) Chem Mater 8:734–743
37. Rulkens R, Tilley TD (1998) J Am Chem Soc 120:9959–9960
38. Wei D, Wang H, Feng X, Chueh W-T, Ravikovitch P, Lyubovsky M, Li C, Takeguchi T, Haller GL (1999) J Phys Chem B 103:2113–2121
39. Gao X, Fierro JLG, Wachs IE (1999) Langmuir 15:3169–3178
40. Gao X, Wachs IE (2000) J Phys Chem B 104:1261–1268
41. Weber RS (1995) J Catal 151:470–474
42. Dzwigaj S, Matsuoka M, Franck R, Anpo M, Che M (1998) J Phys Chem B 102:6309–6312
43. Shul'pin GB, Kozlov YN, Nizova GV, Süss-Fink G, Stanislas S, Kitaygorodskiy A, Kulikova VS (2001) J Chem Soc Perkin Trans 2:1351–1371
44. Kozlov YN, Romakh VB, Kitaygorodskiy A, Buglyó P, Süss-Fink G, Shul'pin GB (2007) J Phys Chem A 111:7736–7752
45. Khaliullin RZ, Bell AT, Head-Gordon M (2005) J Phys Chem B 109:17984–17992